

NANO-INDENTATION AND NANO-SCRATCH TESTS

Raymond Hsiao and D. B. Bogy
Computer Mechanics Laboratory
Department of Mechanical Engineering
University of California at Berkeley
Berkeley, CA 94720

ABSTRACT

Nano-indentation and nano-scratch tests were performed to determine the mechanical properties of a wide variety of materials using the point contact microscope (PCM) and the Hysitron tester, which is a new AFM add-on nano-indentation instrument based on a capacitance loading system. The hardness and nano-scratch depth were measured and compared. It was found that the scratch test by the PCM minimizes surface roughness effects and the nano-scratch depth is shown to correlate well with hardness. The results show that the Hysitron tester provides a reliable relative nano-hardness measurement and is therefore applicable to the nanotribology of ultra thin films, such as those encountered in magnetic recording. The mechanical behavior of a variety of materials, both bulk and thin films, were studied using the Hysitron tester, especially their load-displacement curves. The relative hardness of hydrogenated carbon films was measured in terms of the inverse value of the residual indentation depth. The results show that with this approach, relative hardness can be measured using indentation depths as small as 1 nm, and therefore are applicable to overcoats in the 5-10 nm range of thickness. Finally, a novel and as yet unexplained jump in the load-displacement curve of $\langle 100 \rangle$ Si is revealed.

1 Introduction

The need for techniques for studying the mechanical properties of ultra thin films accounts for the continued interest in nano-indentation devices. Hardness is often calculated as the peak applied load divided by the residual area of the indentation at the sample surface. In a conventional microhardness tester, the area of contact is determined by an SEM image of the indentation after the load is removed and then the diagonal lengths are measured on this image. To avoid the lengthy determination of the projected area measurement with accuracy - errors are introduced due to the resolution in the SEM, the surface roughness and the varying elastic contractions that occur after unloading, especially for small indentations, - a nano-scratch test is proposed as an alternative and is carefully evaluated. In addition, a new nano-indentation instrument built by Hysitron is used and the hardness results are compared with the scratch measurements. The Hysitron tester is capable of resolving indentations with depths of only a few nanometers. The instrument continuously records both the indentation load and displacement, and from this data it is possible to derive a variety of mechanical properties such as elastic modulus, yield stress, and hardness. Because of the linear relationship between indentation area and depth, the inverse value of indentation depth can be used for nano-indentation hardness comparison. In order to properly interpret indentation load-displacement data, it is necessary to understand the mechanical behaviors and deformation mechanisms that can occur during indentation. In this report, we document this behavior and outline the mechanisms from the load-displacement curves for different materials.

2 Experiments And Results

A. Nano-Indentation and Nano-Scratch Tests using the Point Contact Microscope

Nano-Scratch tests were conducted using the Point Contact Microscope (PCM) to examine the general scratching behavior of thin films and quantify the relationship between scratch depth and hardness for purposes of materials comparison. A diamond tip was used to make the scratches in a face-forward direction. During each nanoscratch experiment, the diamond tip with nominal radius of 100 nm was controlled to scan and scratch the samples in three steps. The first step, called the initial scan, was performed at a light load of 10 μN and was used to image the local topography of the sample without damaging the surface. After the initial scan, a 1 μm long scratch was made by applying a heavier load just before the sample was laterally displaced at a velocity of about 1 $\mu\text{m}/\text{sec}$. A third scan, again at the constant light load of 10 μN and referred to as the post-scratch scan, was then made to assess the changes in the surface profile resulting from the scratch. A cross-sectional image of a scratch test on a NiP substrate along the scratch direction is shown in Fig. 1. The uniform depth along the scratch direction provides a clear picture for measurement and comparison. At 120 μN load, three independent scratches on Si with depths of 5.08 nm, 5.01 nm and 4.97 nm, as shown in Fig. 2, indicate the repeatability of the test. To evaluate the correlation between nano-scratch and nano-indentation hardness tests, we performed nano-scratch and nano-indentation tests on a group of eleven SiC samples

designated A, B1, B2, B3, B4, C, D, E, F, G, and H using the PCM. The nano-indentation using the PCM^{1,2} uses the same tip to first indent the surface under a well controlled load and then scan the surface to image the indentation¹ (Lu et al, 1994). With the high resolution of the PCM, better than one nanometer, the residual indentation area can be measured. The hardness is defined as the ratio of the load to the projection area of the residual indentation. In these investigations, a diamond tip with nominal radius of 60 nm was attached to a single parallel-leaf cantilever beam. The films were deposited on silicon substrates with thicknesses in the a range from 230 to 560 nm. Bare silicon was also measured to provide a base for the comparison of the results. For each sample, three nano-indentation tests with a load of 185 μN and two nano-scratch tests with a load of 190 μN were performed and investigated to produce repeatability of the results. A comparison of the nano-indentation and nano-scratch test results is shown in Fig. 3, where the left side Y-axis gives the hardness values for the nano-indentation tests and the right side Y-axis gives the inverse values of nano-scratch depth for the nano-scratch tests. Significant variations of hardness values are observed between samples B1, B2, B3 and B4 that came from the same preparation and are expected have about the same values. The differences are believed to be due to difficulties in determining the indentation areas because of the surface roughness involved. As shown in Fig. 3, the nano-scratch test has a strong correlation to nano-indentation hardness test and therefore it also provides a convenient and reliable way to characterize protective overcoats. With a mere 3.5% difference of nano-scratch depths for samples B1, B2, B3 and B4, we conclude that the nano-

scratch test reduces the effect of surface roughness and is a good alternative to indentation for getting the relative hardness characteristics of thin films.

B. Nano-indentation Tests with the Hysitron Tester

Nano-indentation experiments on the same group of SiC samples were performed using the Hysitron tester, a schematic illustration of which is shown in Fig. 4. The system is a portable add-on to commercially available AFM's and performs nano-indentations with load-displacement curves. It also provides AFM resolution surface imagings, allowing the test region to be aligned over the exact region of interest. The instrument uses a capacitive force/displacement transducer made by Hysitron. It generates the loading force and measures both force and displacement. A three-sided triangular diamond tip with a nominal radius of 35 nm was used in these experiments, which were performed using a triangular load-time profile. The indenter was first loaded linearly to the peak value set up by the user, and then it was unloaded with the opposite load/time slope after a certain total time duration of about 10 seconds. After the test, the load-displacement curve and resulting surface image of the indentation mark were carefully examined to establish a method for determining relative nano-indentation hardness on all of the samples. For each material, two independent tests with the same peak load at 68 μN were performed and investigated to insure repeatability of the results. To evaluate its performance of the Hysitron tester the nano-indentation tests are compared in Fig.5 with the nano-scratch test results that were presented in the previous section. In Fig.5, the left side Y-axis gives the inverse value of residual depth for the nano-indentation tests and the right side Y-axis gives

the inverse value of scratch depth for the nano-scratch tests. The results demonstrate that the Hysitron tester provides a quite reliable means for relative hardness analysis with indentation depths in the range of several nanometers for studying the elastic and plastic properties of thin films. This procedure for determining the relative hardness is also attractive because it does not require imaging and calculation of the projected area of the indentation.

C. General characteristics of the Hysitron load-displacement curves

We begin the discussion of the experimental results with an overview of the characteristics of the load-displacement curves for a second group of samples. The materials used in this study were chosen to span a wide range of mechanical properties. They included SiO_2 , SiC , Si_3N_4 and C. All experiments were performed using a triangular load-time profile. The load versus indenter displacement data are shown in Fig. 6. It can be seen that linear unloading, which implies constant contact area, is observed for the first 1/5 of the unloading from the maximum load. The loss of contact with the indenter results in the deviation from linearity that occurs when the elastic displacements are recovered. The differences in elastic modulus and hardness of the materials are apparent from the large differences in the depths attained at maximum load, 300 μN . The softest material is SiO_2 , with a residual depth of about 22 nm, while the stiffest and hardest is C, which was penetrated to a maximum depth of only about 30 nm. The materials show varying degrees of elastic recovery during unloading, the largest being that for Si_3N_4 . Elastic recovery rate is defined as the ratio of the elastic recovery, which was calculated by subtracting the residual depth from

the maximum depth, to the maximum depth. Thus an elastic recovery rate of 1 represents perfectly elastic behavior in the indentation test. The recovery rates of this group of samples are plotted in Fig. 7, which shows that the load-displacement behaviors of C and Si₃N₄ are largely elastic while SiO₂ is the most “plastic” sample in this group with a recovery rate of only 0.6. It is noted that the elastic and plastic properties of the samples are quite different. For example, in Fig. 6 it is seen that Si₃N₄ has a maximum depth of about 96.5nm, but it has a residual indentation depth of only about 10 nm. A third group of samples, of three different carbon films, designated 1051, 1052 and 900 and two ZnO films designated N and S2, were also examined to establish a better understanding and an expanded view of the unloading behavior for different materials. As shown in Fig.8, the carbon films that are commonly used for overcoat protection in magnetic hard disks exhibit a predominantly elastic behavior during the deformation. The indenter displacement of the ZnO sample is accommodated plastically and only a small portion, about 35%, is recovered on unloading. The carbon films, samples 1051, 1052 and 900, had about the same recovery rate, however, sample 900 had a significantly smaller residual depth.

D. Nano-indentation on silicon

Recently, we have been characterizing and cataloging the wear mechanisms and indentation load-displacement characteristics of a large variety of materials. During the course of this work, it has become evident that the nano-fatigue wear and load-

displacement behavior of silicon is different from that of most other materials. Load-displacement curves for indentation tests performed in different load ranges on Si that has been exposed to ambient environment for an extended period of time are shown in Fig. 9. This is single-crystalline, p-type silicon with a $\langle 100 \rangle$ orientation. The indenter was loaded onto the specimen at a constant loading rate to a pre-determined peak load and then unloaded at the same rate. These indentations were produced with peak loads of 9.7 μN , 28.5 μN and 47.8 μN and at loading rates of 2.86 $\mu\text{N/s}$, 8.38 $\mu\text{N/s}$ and 14.08 $\mu\text{N/s}$, respectively. An unusual feature for indentations with peak load greater than 20 μN is the clear, reproducible discontinuity in displacement on the loading curves that occurs near 18 μN . Apparently, as the indenter is loaded, a perfectly plastic response occurs at initial yield allowing the indenter to displace about 2 nm at constant load. When the peak load is only about 10 μN , the loading and unloading curves exactly overlay each other, indicating that all of the deformation is elastic. The same loading “kink” phenomenon is observed at larger peak loads such as 70 μN and 90 μN . It should be noted that similar behavior is not observed when the indentations are made on p-type silicon with a $\langle 111 \rangle$ orientation. Similar experimental results have been reported by Pethica and Tabor for nickel^{3,9}, Oliver and Pharr for tungsten⁴ and Venkataraman, et al. for iron⁵. Such displacement excursions during indentation have been attributed by some authors to oxide breakthrough by dislocations or a contamination effect. The loading displacement discontinuity observed here is a phenomenon quite unique to silicon. Of the approximately 25 materials we have indented in the past year, silicon is the only one to exhibit this behavior. One contributing factor may be an oxide layer or contamination on the

surface of the silicon due to the long exposure to the laboratory environment. On the other hand, Pharr, et al.⁶ presented and discussed the behavior of a loading “kink” on germanium and a “unloading” discontinuity on silicon and suggested that it is probably due to radial cracking during loading for the case of germanium. An interesting aspect about this load-displacement characteristic is found by comparing it to that of the same Si<100>, but cleaned with HF(hydrofluoric acid), and using the same tip. Fig. 10 presents the comparison, from which it is seen that the load-displacement behavior of the “clean” silicon is significantly different from that on the original one. The loading discontinuity is not present, and in its place is a smooth loading curve that continues toward the pre-determined peak load with its first 8 nm displacement entirely coincident with that of the original silicon. This phenomenon can not be readily explained by the above suggestions since the radial cracks may not be easily avoided by HF, and the removal of an oxide or contamination layer is not consistent with the initial overlay of the two curves in regions nearest the surface. Why the discontinuity is observed only in silicon, only on one orientation, and disappears after the silicon is cleaned with HF is still not understood.

E. Independence of loading history

To explore the possibility that different loading profiles may cause changes of indentation behavior, a series of test with distinct loading profiles were performed at the same pre-determined peak load on the “clean” Si<100> sample using the same tip. Fig.11 shows the three different loading profiles; triangle, trapezoid and rectangle,

with different loading/unloading rates and total time duration, but with the same peak load. As shown in Fig.12, no differences in load-unload behavior were observed as their maximum and residual depths are about the same, suggesting that the loading profile, including loading rate, is not an important variable.

F. CH_x coatings with different hydrogen levels

It is well known that the effect of the substrate is not significant if the indentation depth is smaller than about one fifth of the film thickness depending also on the materials and the ratio of tip radius to layer thickness, Lu and Bogy⁷. Hence, it is acceptable to compare the hardnesses of the different films without significant influence of the substrates using the results obtained with residual indentation depths less than one fifth of the film thickness. Keeping this 1/5 rule in mind, one question which remains to be answered is how small the indentation needs to be to provide enough information for comparison with a particular tip radius, since indentations that are too small on thin films will obviously not be resolvable with sufficient accuracy. Recent studies¹⁰ have shown that the hardness of hydrogenated-carbon films decreases with the increase of hydrogen content. Indentations were made on hydrogenated-carbon films 2A and 3A, with 3A having a higher hydrogen concentration. For each sample, fifteen separate peak loads were investigated starting at 500 μN and successively reducing the peak load by 50 μN until 100 μN , and then 10 μN until 10 μN , to produce indentations. Two indentations were made at each load, and the results are presented in Fig. 13, representing averages of the two tests. One advantage of determining the relative hardness by comparing their residual

depths resulting from indentations with the same peak load and the same tip is that it eliminates the surface roughness effect on the determination of projected area and the indenter geometry. In studying a large number of indentations on these 100 nm thick CH_x coatings using a diamond tip with a 50 nm radius, it is revealed that relative hardness can be measured accurately enough with residual depths as small as 1 nm. One feature which plays a key role in improving the reliability of relative hardness comparisons for thin films is the tip radius, especially for the case of a hard layer on a relatively soft substrate. Thin film measurements are also sensitive to the tip radius, and it has been shown in Lu and Bogy⁸ that the tip radius to layer thickness ratio should be less than 1.25. Therefore, with current advances in diamond tip manufacturing, relative hardness measurements on several nanometers thick films are not out of reach.

3. Conclusions

1. Nano-scratch test results correlate well with the nano-indentation hardness test results using the PCM and, in fact show less sensitivity to surface roughness effects.
2. The Hysitron tester provides an excellent means for studying the mechanical properties of thin films. This instrument gives good correlation with the nano-scratch hardness and is able to resolve indentations with residual depths as small as one nanometer.
3. Residual depths have been compared from the indentation load-displacement data for a variety of samples with the same pre-determined peak load. Comparison of

relative hardness by this new procedure with values measured independently by nano-scratch test using the PCM shows that this procedure is a good measure of relative hardness.

4. Careful examination of the indentation load-displacement data obtained using the Hysitron tester reveals that during the deformation there are substantial differences in the mechanical properties that can be valuable to the performance of the thin films as protective overcoats.

5. The load displacement curves for silicon<100> exhibit a discontinuity in the loading curve, but they do not show this loading “kink” after the silicon is cleaned with HF.

6. The loading profile, including loading/unloading rate, is not an important variable for determining mechanical properties in nano-indentation tests of the materials tested here.

7. The finest resolution of the new approach for relative hardness measurement by comparing the residual depth using the Hysitron tester on 100 nm thick CH_x coatings is about 1 nm.

List of Figures

Fig.1. Section view of nano-scratch test on NiP substrate.

Fig.2. Section view of 3 independent scratch tests on Si<100> .

Fig.3. The comparison of nano-indentation and nano-scratch test results.

Fig.4. Schematic diagram of the Hysitron tester.

Fig.5. The comparison of nano-indentation using the Hysitron tester and nano-scratch test using the PCM.

Fig.6. Load-Displacement curves of nano-indentation test on the second group of sample using the Hysitron tester.

Fig.7. The recovery rates of the second group samples.

Fig.8. The recovery rates of the third group samples.

Fig.9. Load-Displacement curves of nano-indentation tests on Si<100>.

Fig.10. Comparison of the load-displacement curves for original and “cleaned” Si<100>.

Fig.11. Three different loading profiles used to indent on “clean” Si<100>.

Fig.12. Maximum and residual depths of nano-indentation with different loading profiles.

Fig.13. Residual depth vs. load in nano-indentation tests on hydrogenated carbon films.

References

1. C.J. Lu, D.B. Bogy and R. Kaneko, *ASME J. Tribology*, 116, 175 (1994)
2. R. Kaneko, N. Nonaka, and K. Yasuda, "Summery Abstract: Scanning Tunneling Microscope and Atomic Force Microscope for Microtribology", *J. Vac. Sci. Technol. A*, Vol. 6, No. 2, pp. 291-292, 1988.
3. J.B. Pethica and D. Tabor, *Surf. Sci.* 89, 182 (1979)
4. W.C. Oliver and G.M. Pharr, *J. Mater. Res.* 7, 1564 (1992)
5. S.K. Venkataraman, D.L. Kohlstedt and W.W. Gerberich, *J. Mater. Res.* 8, 685 (1993)

6. G.M. Pharr, W.C. Oliver and D.R. Clarke, *J. Elec. Mater.* 19, 881 (1990)
7. C.-J. Lu and D.B. Bogy, "Sub-microindentation hardness tests on thin film magnetic disks", *Advances in Information Storage Systems*, Vol. 6, pp. 163-175.
8. C.-J. Lu and D.B. Bogy, The effect of tip radius on nano-indentation hardness tests", *Int. J. Solids and Structures*, Vol. 32, 12, 1759-1770, 1995.
9. N.A. Stilwell and D. Tabor, *Proc. Phys. Soc.* 78, 169 (1961)
10. Z. Jiang, C.-J. Lu, D.B. Bogy, C.S. Bhatia, and T. Miyamoto, 1995, "Nanotribological characterization of hydrogenated carbon films by scanning probe microscopy", *Thin Solid Films*, Vol.258, pp. 75-81.

Acknowledgments

This research was supported by the Computer Mechanics Laboratory at the University of California at Berkeley. We are indebted to Hysitron for providing their tester for our use.

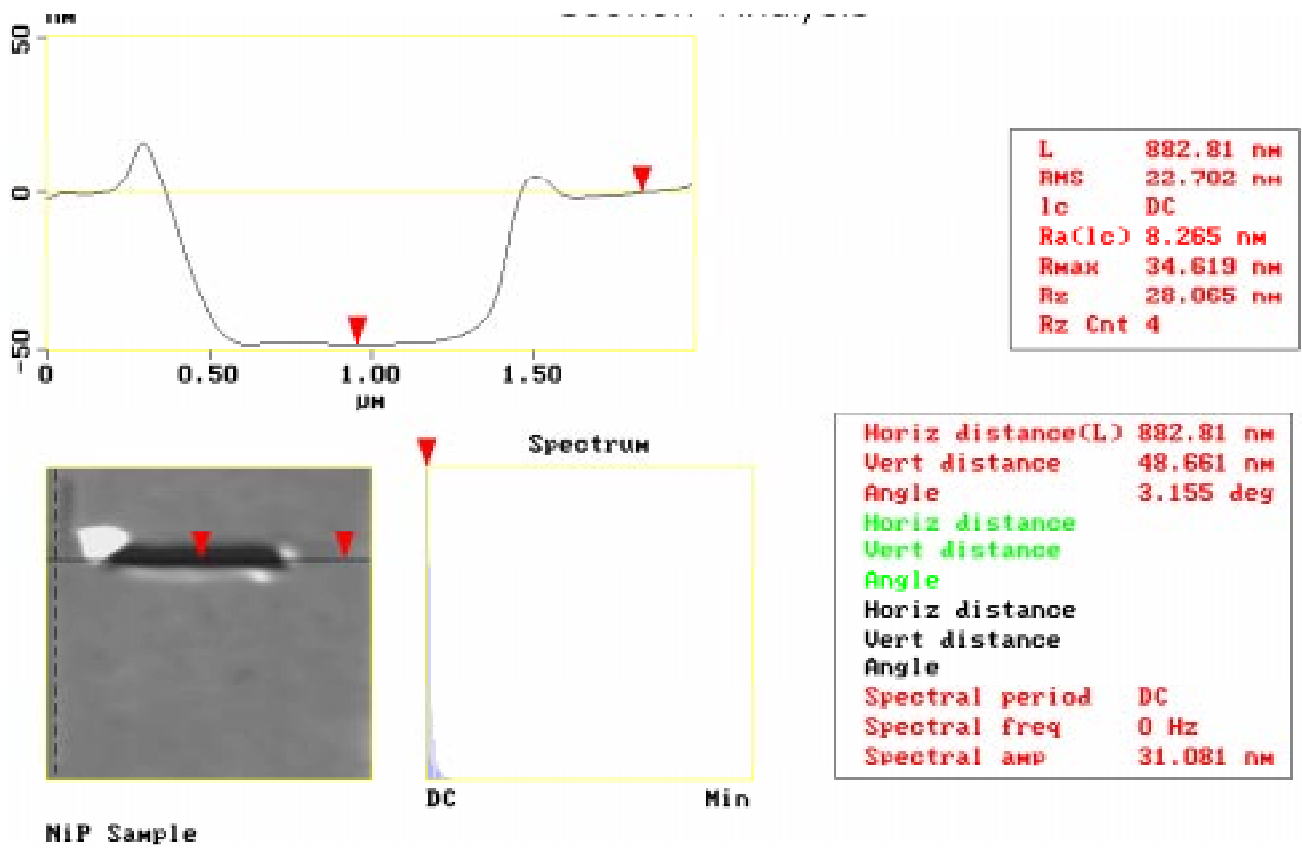


Fig. 1. Section view along the scratch direction of nano-scratch tests on NiP substrate.

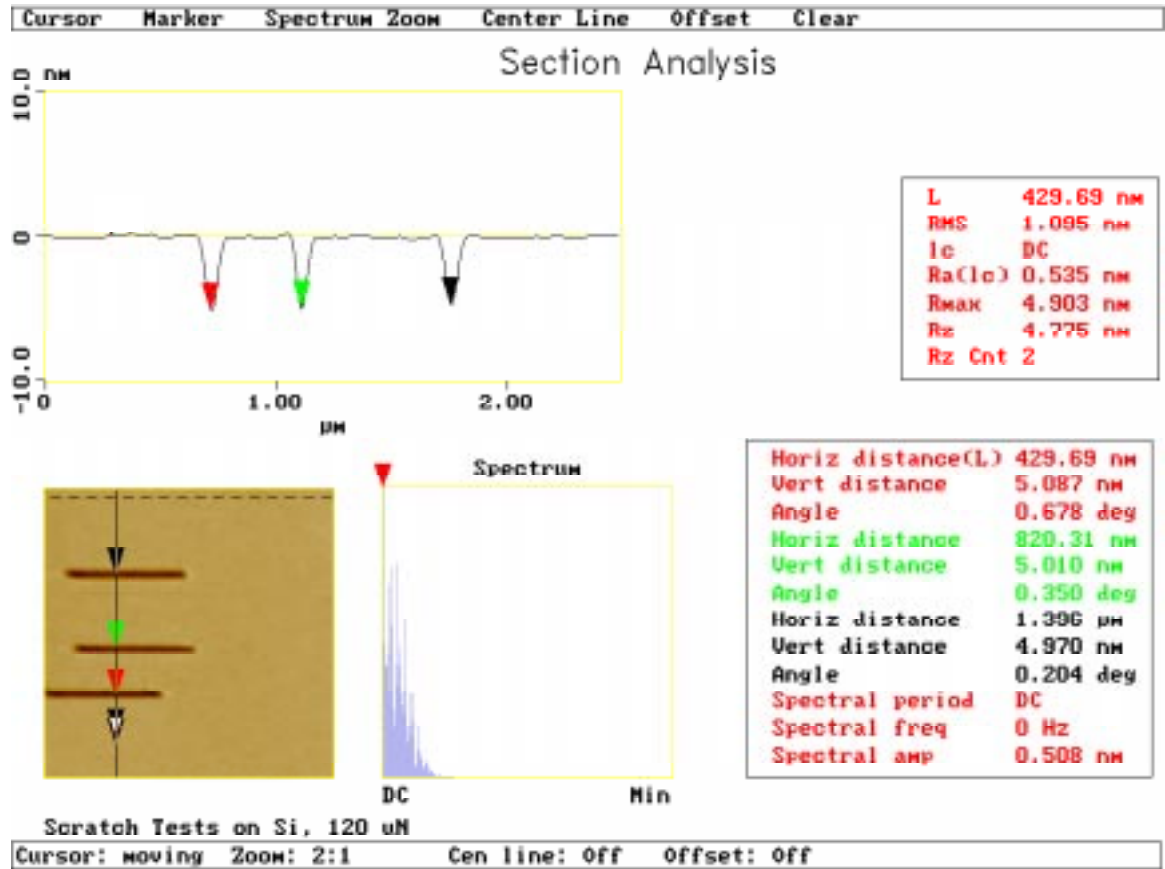


Fig. 2. Section view of 3 independent scratch tests on Si<100>.

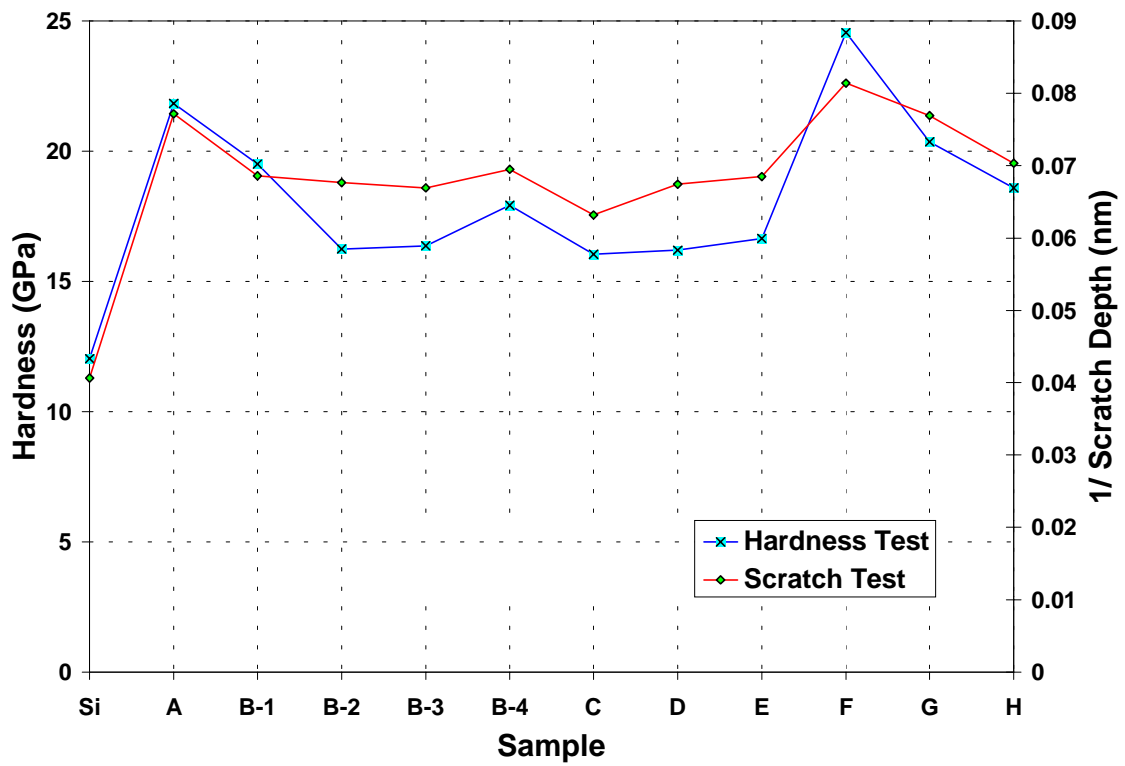


Fig. 3. Comparison of nano-indentation and nano-scratch test results using the PCM.

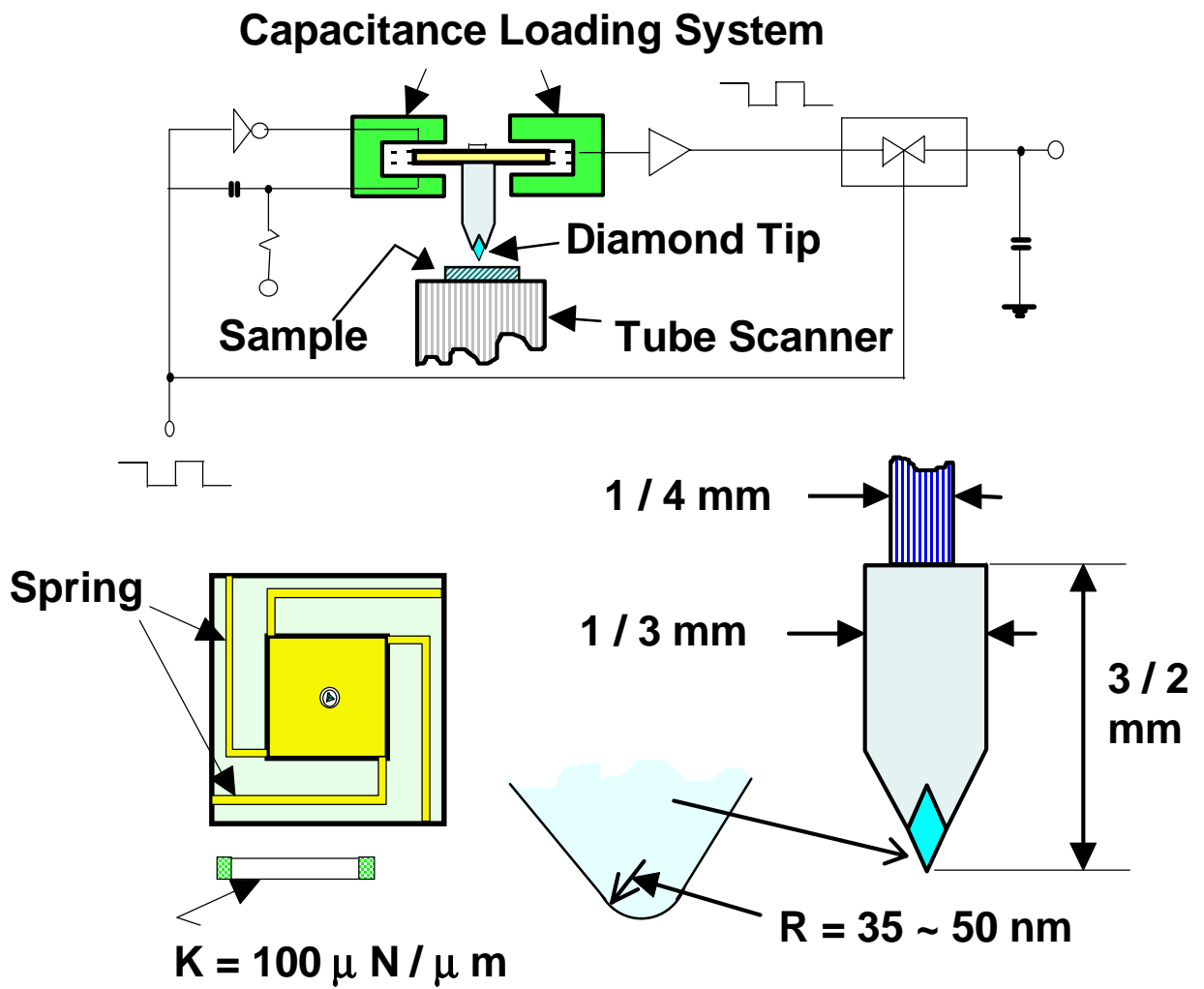


Fig.4. Schematic diagram of the Hysitron tester.

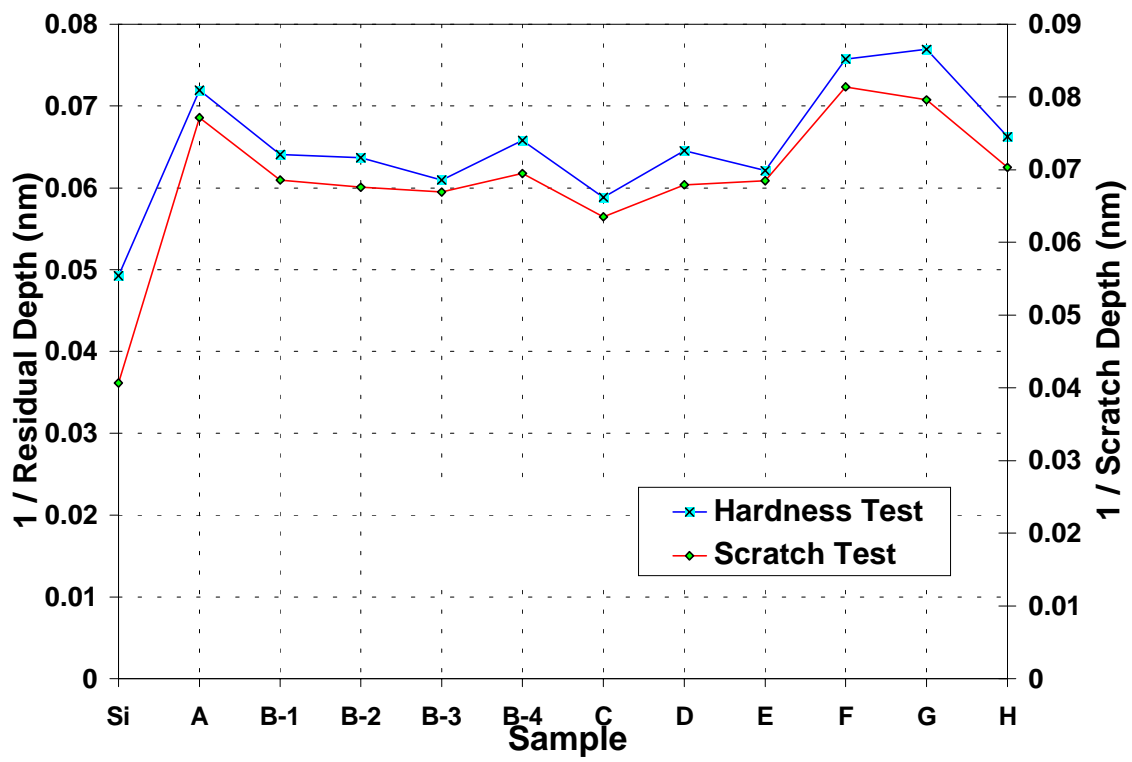


Fig.5. Comparison of nano-indentation results using the Hysitron tester and nano-scratch test results using the PCM.

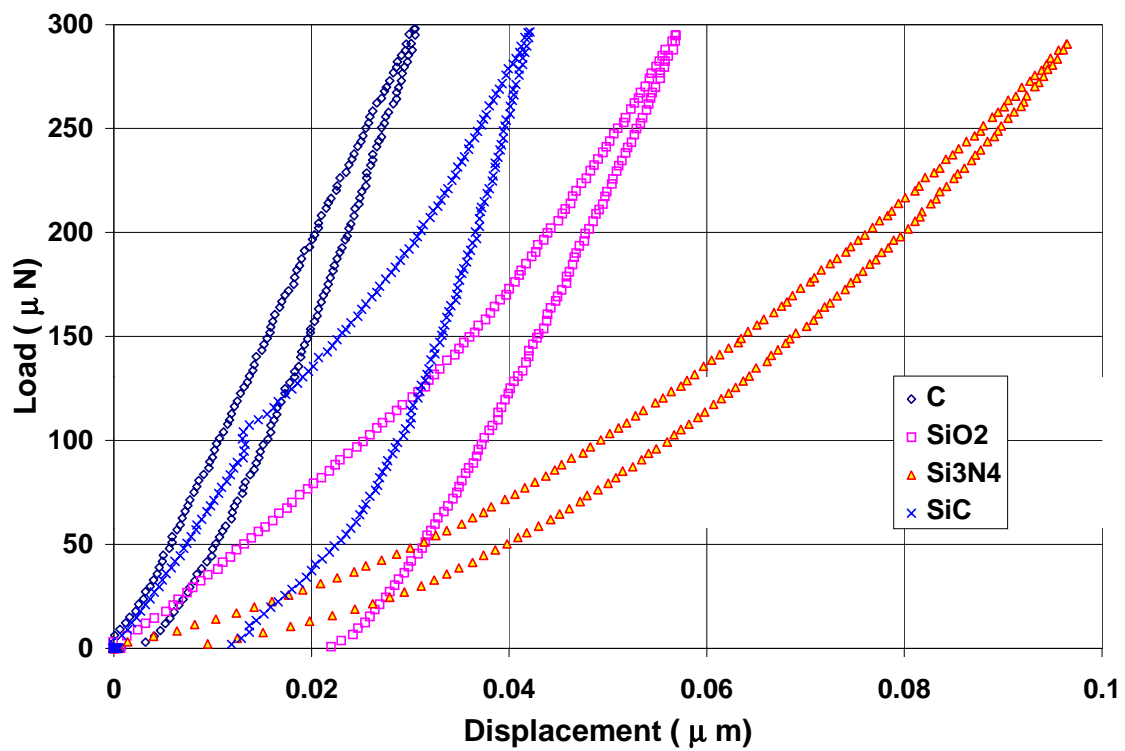


Fig.6. Load-displacement curves of nano-indentation test on the second group samples using the Hysitron tester.

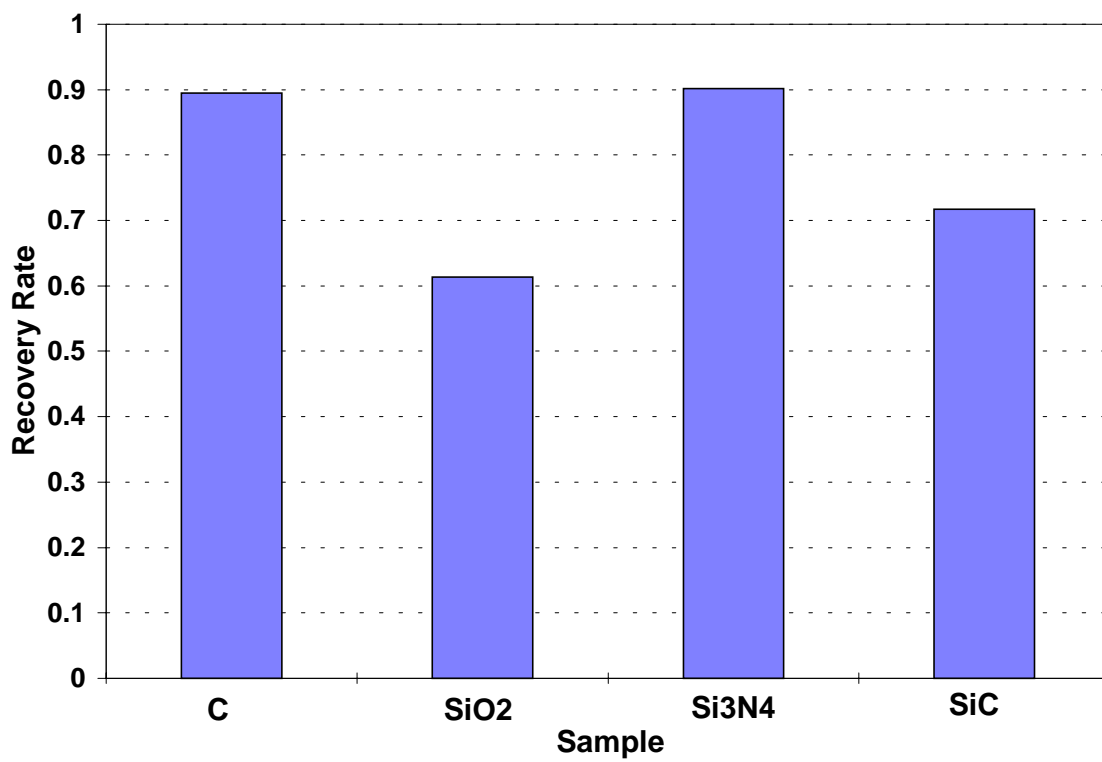


Fig.7. The recovery rates of the second group samples.

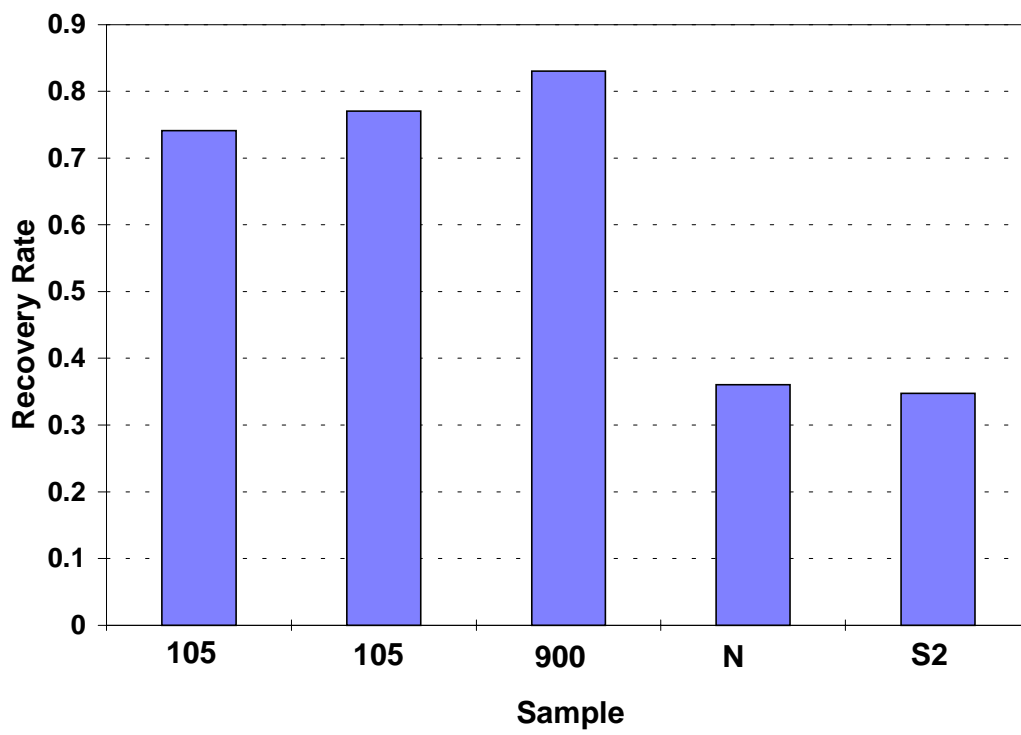


Fig.8. The recovery rates of the third group samples.

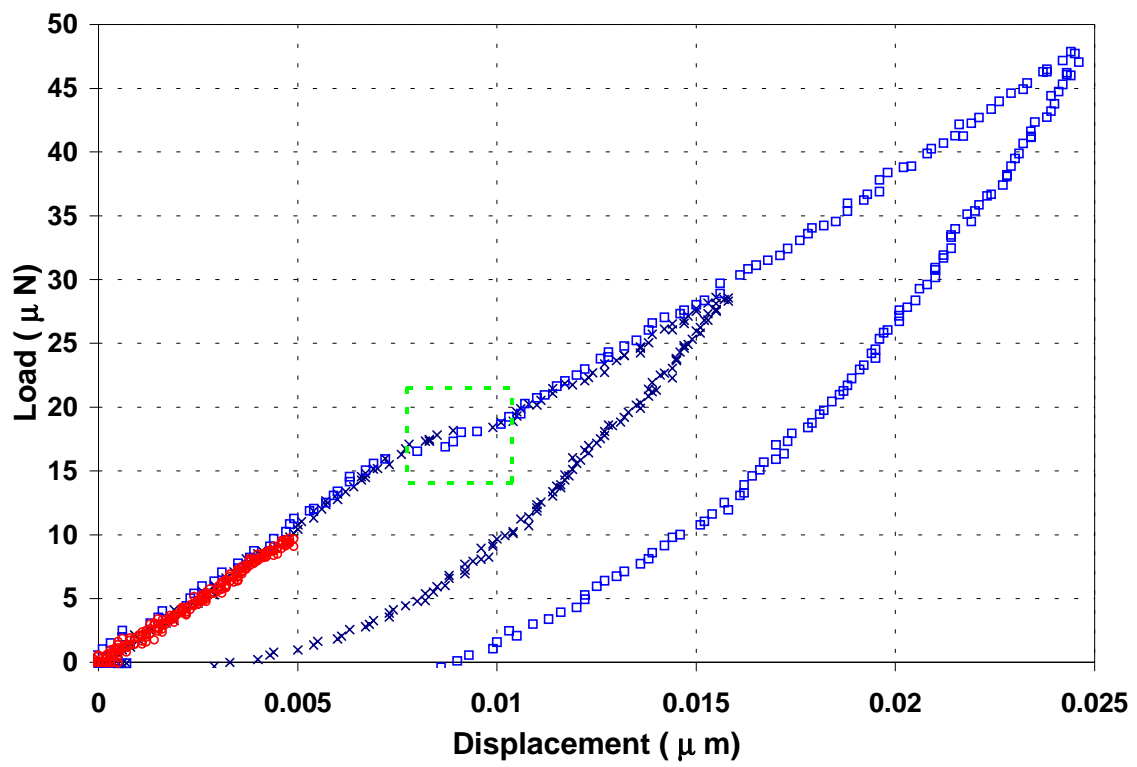


Fig.9. Load-displacement curves of nano-indentation tests on Si<100>.

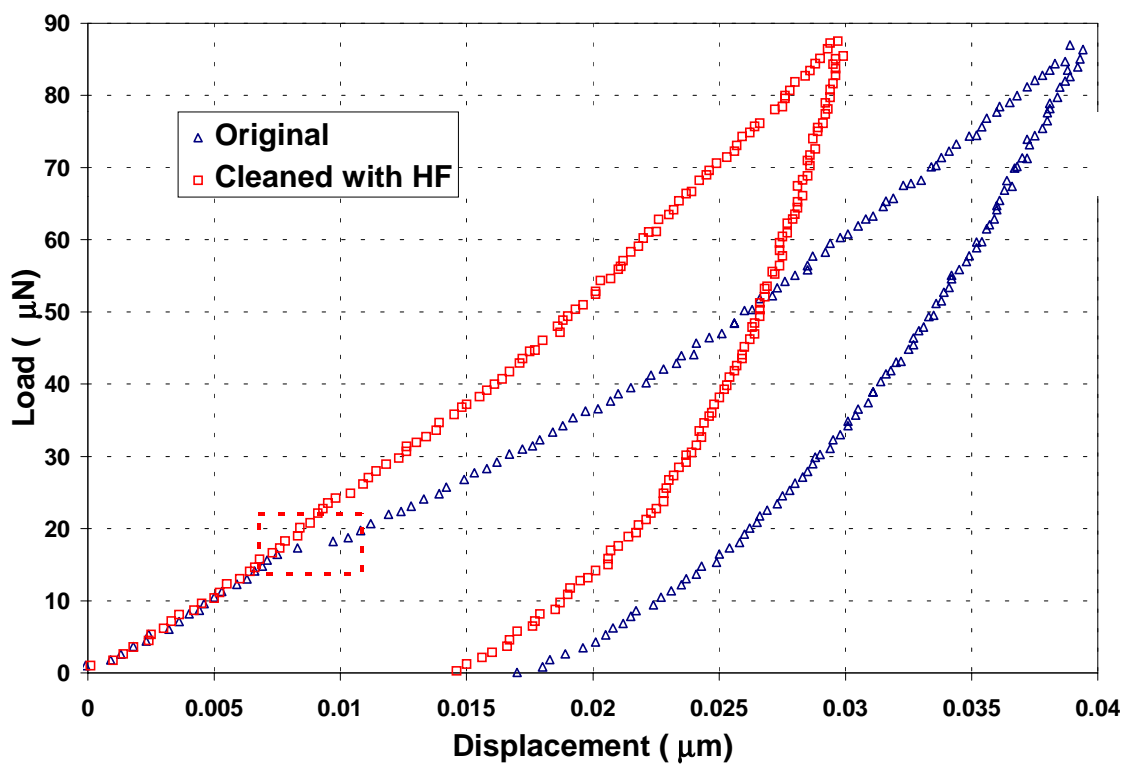


Fig.10. Comparison of the load-displacement curves for original and "cleaned" Si<100>.

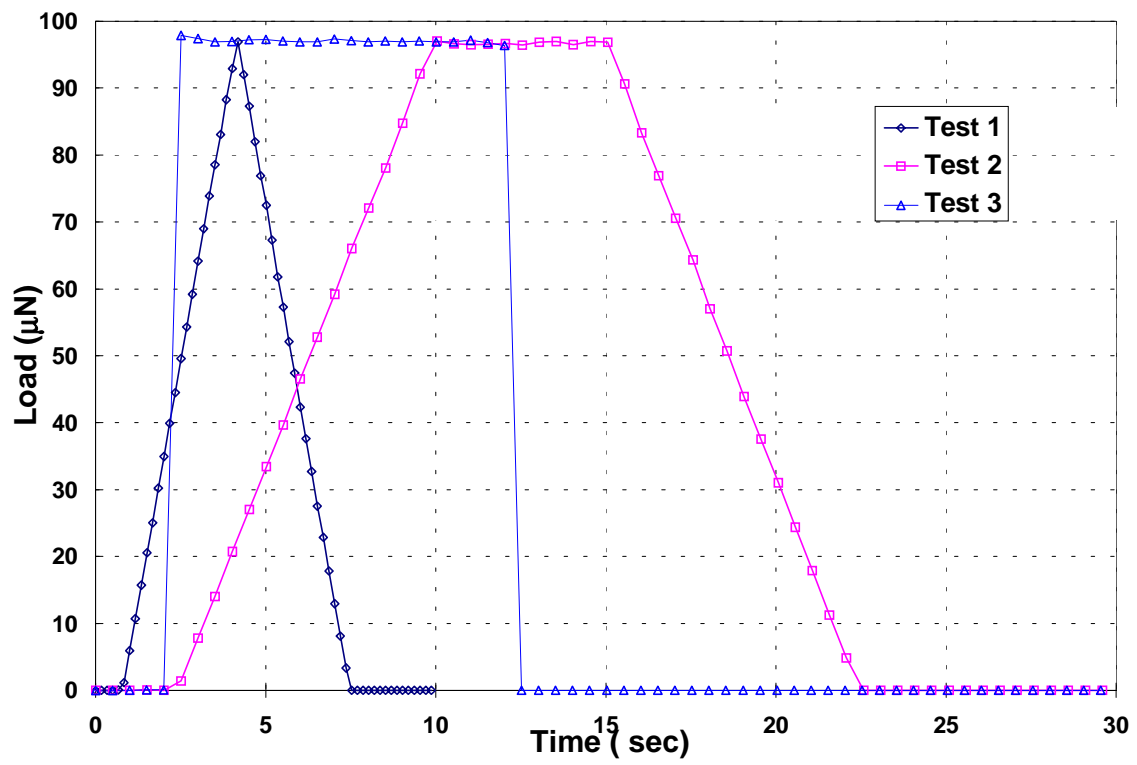


Fig.11. Three different loading profiles used to indent on "clean" Si<100>.

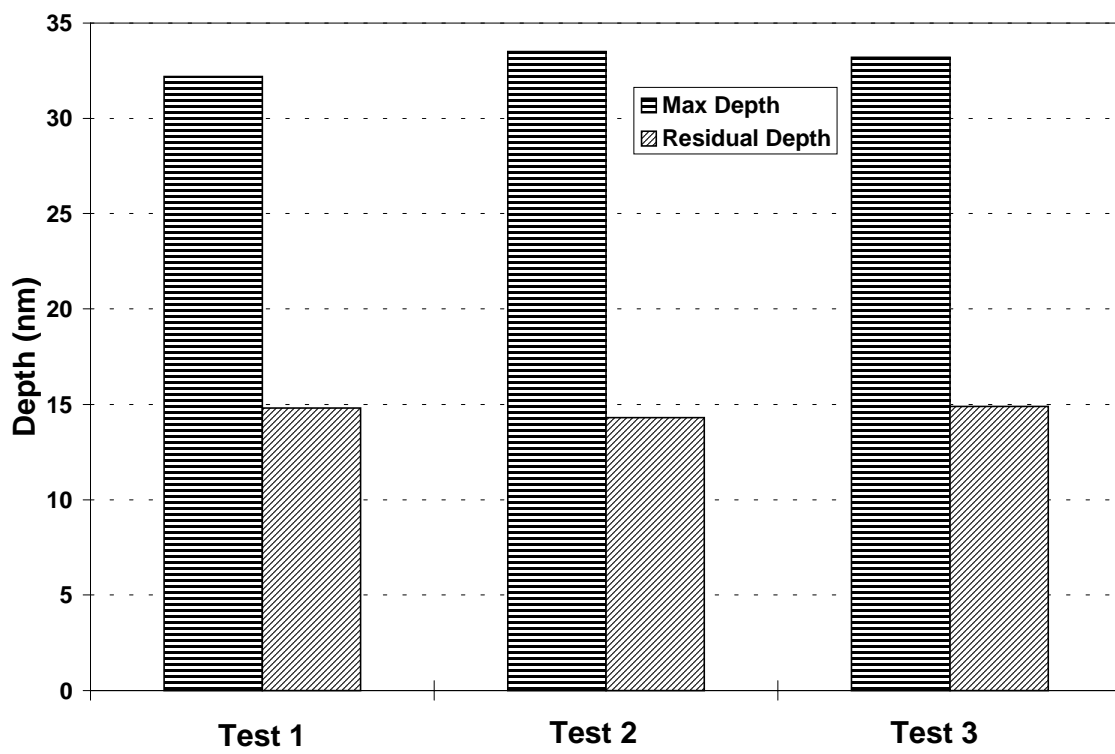


Fig.12. Maximum and residual depths of nano-indentation on Si<100> with different loading profiles.

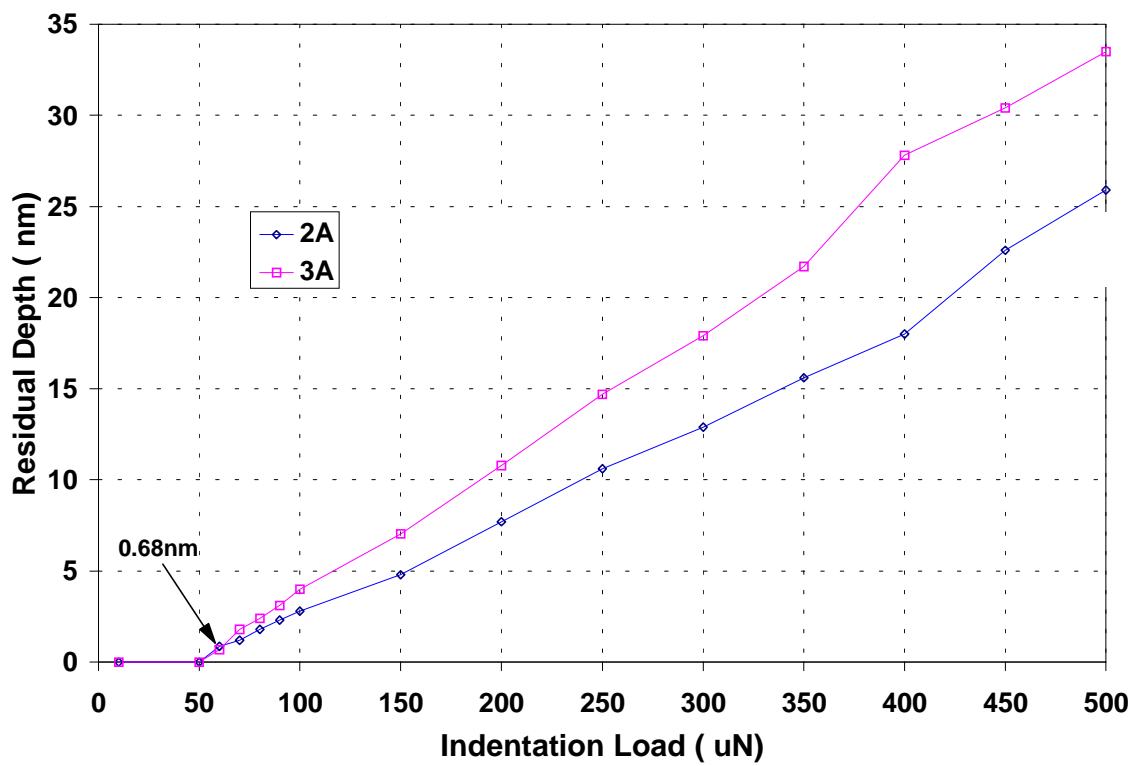


Fig.13. Residual depth vs. load in nano-indentation tests on hydrogenated carbon films.